Critical Size and Anomalous Lattice Expansion in Nanocrystalline BaTiO3 Particles

doi: 10.1103/PhysRevB.62.3065

Critical size and anomalous lattice expansion in nanocrystalline $BaTiO_3$ particles

S. Tsunekawa,[1] S. Ito,[1] T. Mori,[2] K. Ishikawa,[2] Z.-Q. Li,[3] and Y. Kawazoe[1]
[1]*Institute for Materials Research, Tohoku University, Sendai 980-8577, Japan*
[2]*Research Institute of Electronics, Shizuoka University, Hamamatsu 432-8011, Japan*
[3]*Steacie Institute for Molecular Sciences, National Research Council of Canada, 100 Sussex Drive, Ottawa, Ontario, Canada, K1A OR6*
(Received 18 February 2000)

Nanocrystalline barium titanate particles are prepared by the alkoxide method. The lattice constants are obtained from the electron diffraction patterns for various orientations of single particles in the size range of 15–250 nm in diameter. The present result indicates that the structural change from a tetragonal (ferroelectric) phase to a cubic (paraelectric) one occurs around 80 nm in diameter, which is in good agreement with a critical diameter recently reported. Large lattice expansions of more than 2.5% are detected in the particles down to 15 nm in diameter. The origin of the expansion is discussed on the basis of x-ray photoelectron spectroscopic analyses and a computer simulation.

I. INTRODUCTION

Most technologically important ferroelectrics are oxides with a pervoskite structure,[1] because that structure has a wide capacity characterized by a tolerance factor.[2] Barium titanate ($BaTiO_3$) is the best studied material among ferroelectric pervoskites, not only for bulk crystals[3] and films[4] but also for nanosize particles.[5–12] For $BaTiO_3$ nanoparticles, the critical size below which the crystal structure changes from a tetragonal phase to a cubic one with no spontaneous polarization has been reported to be from 9 to 110 nm. In addition, a large lattice elongation was observed in the ferroelectric phase near a critical size of ~10 nm.[12] However, almost all of the studies were carried out indirectly for aggregated nanoparticles by x-ray diffraction.

In the present paper, we report on the critical size and lattice expansions directly observed in nanocrystalline $BaTiO_3$ single particles in the size range from 15 to 250 nm in diameter by transmission electron microscope (TEM). We discuss the critical size and the origin of the lattice expansion, which increases with decreasing particle size, according to x-ray photoelectron spectroscopy (XPS) for the respective constituent ions and a computer calculation on the structure of clusters.

II. EXPERIMENTS

A. Sample preparation and TEM observation

Nanocrystalline specimens were prepared from ultrafine $BaTiO_3$ particles obtained from hydrolyzing the mixture of two constituent alkoxides,[13] by heating at various temperatures (T) and for various time periods (H): $C1$ ($T=673$ K, $H=1$ h), $C2$ ($T=1073$ K, $H=96$ h), $C3$ ($T=1373$ K, $H=25$ h), and $C4$ ($T=1443$ K, $H=2$ h). The specimens were ultrasonicated in ethanol for 300 s. $C1$ and $C2$ specimens were then left undisturbed for more than 4 h but $C3$ and $C4$ specimens for less than 600 s, after which a drop of each supernant liquid was put on a microgrid used for TEM, in order to sample only the colloidal part. Bright field images and diffraction patterns of isolated single particles were obtained using a 20-kV TEM (JEM-2000FX, JEOL) with an energy dispersive x-ray (EDX) spectrometer. All the particles had atomic ratios of Ba/Ti between 0.99 and 1.01 in the EDX analysis.

B. Computation and XPS measurement

Model calculations of the interatomic distance for small particles were performed by a cluster model using *ab initio* ultrasoft pseudopotentials with a plane-wave basis.[14] The exchange-correlation potential was treated with the generalized gradient approximation by Perdew.[15] The systems were relaxed until the forces on each atom were estimated to be less than 0.01 eV/Å.

XPS measurements were performed with a commercial apparatus (SSX-100, Surface Science Instruments). Four ethanol suspensions of $BaTiO_3$ nanoparticles obtained from the specimens $C1$, $C2$, $C3$, and $C4$ were dropped and dried on Ag plates. Size distributions in the suspensions were estimated by a commercial dynamic light scattering apparatus (LPA-3000/3100, Otsuka Electronics Co.) as $D'1=19\pm3$, $D'2=45\pm9$, $D'3=110\pm25$, and $D'4=350\pm80$ nm in diameter, respectively, where the range indicates the standard deviation of the particle diameter. The XPS spectra were recorded in the binding energy range from 0 to 1200 eV using the monochromated Al Kα line (1486.6 eV) as x-ray source under a pressure of $1-2\times10^{-7}$ Pa.

III. RESULTS AND DISCUSSION

A. Anomalous lattice expansion and critical size

Figures 1(a)–1(d) show electron micrographs of the bright field image obtained for single particles in the above four specimens, $C1$, $C2$, $C3$, and $C4$, as well as diffraction spot patterns for a [001] incident beam. A crystallographic spacing d is estimated by the following equation: $d_{hkl}=L\lambda/s$, where L, the camera length corrected by Au particles as a standard, is 734 mm, λ is the wavelength of electrons at 20 kV, 0.025 08 Å, s is the distance in mm between two diffraction spots, and hkl is the Miller index. The values of lattice constant a obtained from d_{100} and of single-particle

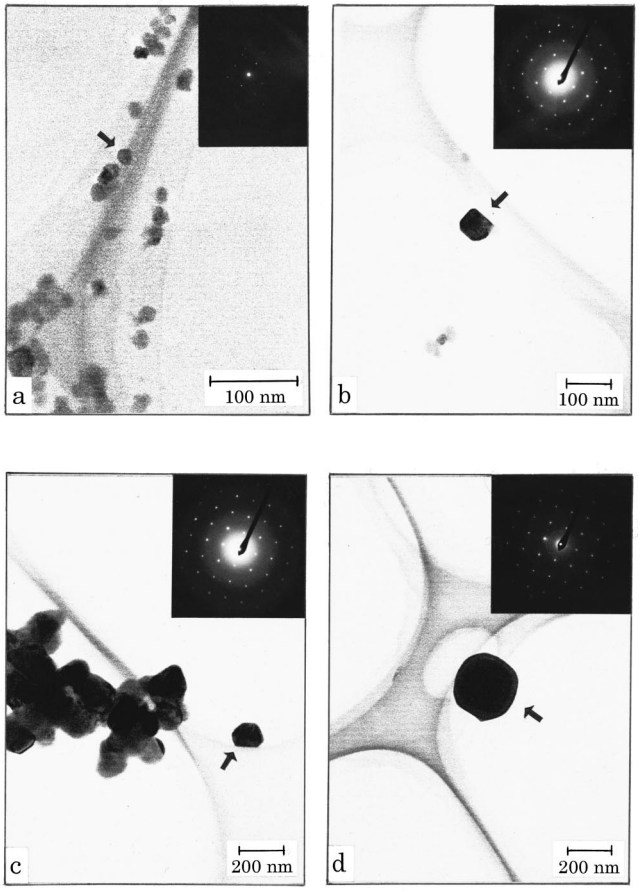

FIG. 1. Electron micrographs for single particles of the diameter, (a) $D1$, (b) $D2$, (c) $D3$, and (d) $D4$. Diffraction patterns were obtained from the (001) plane of the single particles indicated by the arrows.

diameter D converted from the area are $a=4.09\pm0.01$, 4.06 ± 0.01, 4.01 ± 0.01, and 3.99 ± 0.01 Å, and $D1=15\pm1$, $D2=51\pm2$, $D3=114\pm6$, and $D4=250\pm13$ nm in diameter for the $C1$, $C2$, $C3$, and $C4$ specimens, respectively, where the ranges denote the experimental error, determined mainly by the measurement of s. Lattice constants a and c are also obtained from electron diffraction spot patterns for an incident beam perpendicular to (112) by using the equations $d_{110}=a/\sqrt{2}$ and $d_{111}=ac/\sqrt{a^2+2c^2}$: $a=c=4.09\pm0.01$ Å; $a=c=4.05\pm0.01$ Å; $a=4.01\pm0.01$, and $c=4.03\pm0.01$ Å; and $a=4.00\pm0.01$ and $c=4.03\pm0.01$ Å, respectively, for the particle sizes $D1$, $D2$, $D3$, and $D4$. It is considered that the nanoparticles with diameters $D1$ and $D2$ are cubic and those with $D3$ and $D4$ are tetragonal, because the lattice constants a and c of the former are the same within the experimental error, while those of the latter are different, according to the above electron diffraction analysis of d_{100}, d_{110}, and d_{111}. Figure 2 shows the dependence of the lattice constants on the particle size, where closed circles and triangles denote a and c, respectively, for respective single particles obtained from the above result, and open ones for an aggregate (having size distribution of 350 ± 40 nm diameter) taken from the electron diffraction ring pattern.

In the model calculation, clusters composed of 5, 14, and 20 units of $BaTiO_3$ (25, 70, and 100 atoms in the cluster) yielded interatomic distances for Ba-Ti of 3.85, 3.66, and

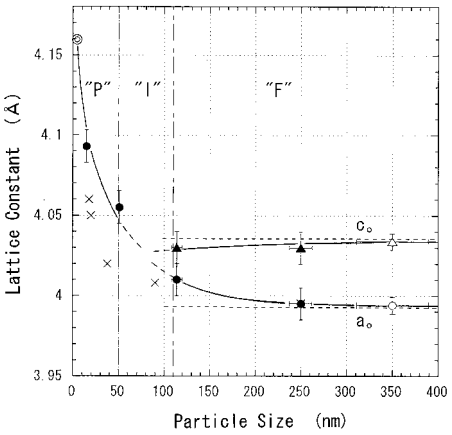

FIG. 2. Dependence of the lattice constant on the particle size, where $a_0=3.9920$ and $c_0=4.0361$ Å are the lattice constants of $BaTiO_3$ bulk crystals: a (●) and c (▲) are those of single particles from the four specimens $C1$, $C2$, $C3$, and $C4$, a (○) and c (△) are those of an aggregate in $C4$, obtained from the electron diffraction patterns, a (◎) is a nominal lattice constant for 20 $BaTiO_3$ units obtained from a cluster model, and a (×) represents the results obtained by Tanaka and Makino (Ref. 12).

3.60 Å, respectively, while it is 3.47 Å in the bulk crystal regarded as a pseudocubic crystal of a lattice constant $a_1=4.0066$ Å: $a_1^3=a_0^2c_0$; $a_0=3.9920$ and $c_0=4.0361$ Å.[16] The cluster composed of 20 $BaTiO_3$ units had a nominal lattice constant of 4.16 Å, which is in good agreement with the previously reported lattice expansion, or lattice relaxation, of 0.15 Å on the $BaTiO_3$ surface,[13] where an estimated cluster, considered as a cube, has a size about 1.1 nm ($4.16\times20^{1/3}$ Å). This calculated value is also consistent with the trend of our experimental results, as shown by a double circle in Fig. 2. It is noted that the simulation result for this oxide is quite different from that for metals, where metal clusters generally have smaller lattice constants than bulk crystals.

It can be seen in Fig. 2 that the lattice constant a increases for particle sizes less than 110 nm diameter, the elongation reaching more than 2.5% in a particle diameter of 15 nm, while the lattice constant c slightly decreases with decreasing particle size down to a critical diameter estimated as 80 nm, which has been named a critical size, as described below. The variation of the lattice constants, therefore, is considered to be divided into three regions according to size. One is a tetragonal F (polar=ferroelectric) phase in the size range above 110 nm diameter. Others are a cubic P (nonpolar=paraelectric) phase for the particles less than 50 nm diameter and an intermediate phase between 50 and 110 nm diameters, I, consistent with the existence of a diffuse phase transition, as is usually found for nanosize crystals, recently called a size-driven phase transition[17,18] or a size-induced diffuse one.[19] But it has not yet been recognized clearly that the lattice parameter a increases rapidly with decreasing particle size after the phase transition. Tanaka and Makino obtained indirectly for the first time such an elongation of a from the x-ray diffraction analysis for aggregated $BaTiO_3$ nanoparticles:[12] the elongation reaches 1.7% for the particles down to 15 nm in diameter in the P phase, as indicated by the crosses in Fig. 2. However, they considered it to be an expansion of a in the ferroelectric phase, because they

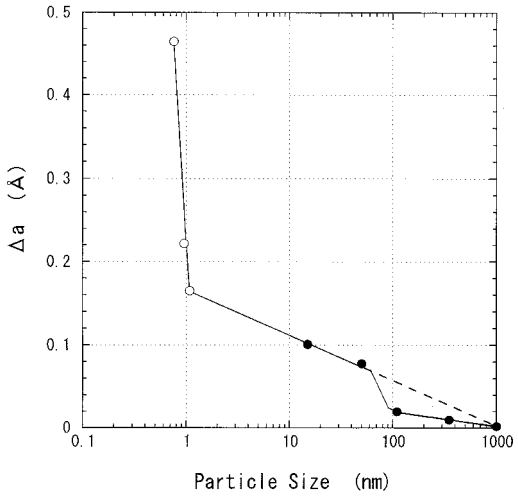

FIG. 3. Semilogarithmic plot of lattice constant change (Δa) versus particle size (D), where $\Delta a = a - a_0$; $a_0 = 3.9920$ Å and the lattice constants a are obtained from nanoparticles (●) and clusters (○) as shown in Figs. 2 and 4, respectively.

estimated the critical size to be about 10 nm. This differs from the present explanation that a moderate expansion happens for the particle of 114 nm diameter, $D3$, (tetragonal) before the I phase and a larger expansion appears in the particle of 51 nm diameter, $D2$ (cubic), after the I phase as shown in Fig. 2. However, nanoparticles having sizes between 50 and 110 nm were rarely found in the present TEM observation, which may be related to the existence of the diffuse phase transition. Hence, we estimate roughly that the critical size is an average between the two sizes.

Figure 3 shows a semilogarithmic plot of Δa vs D, where $\Delta a = a - a_0$ and a_0 is a lattice constant of $BaTiO_3$ bulk crystals at 293 K, 3.9920 Å,[16] where the lattice constant of clusters was estimated with the interatomic distances Ba-O and Ti-O shown in Fig. 4. The present result strongly suggests that a characteristic expansion (volume inflation) or lattice

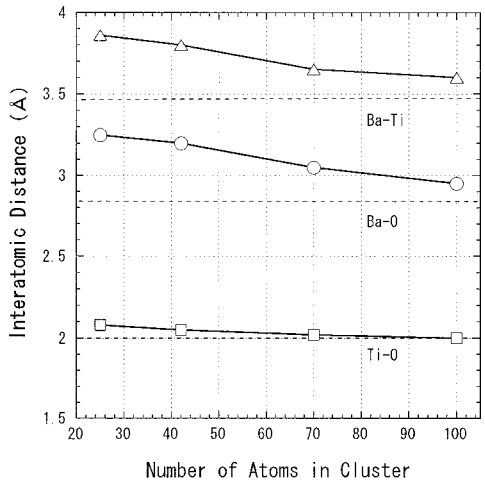

FIG. 4. Plot of interatomic distance versus number of atoms in cluster estimated by a cluster model, where vibrational changes of the interatomic distance depending on the cluster size are averaged. Dashed lines represent interatomic distances in the bulk crystal of 3.47, 2.83, and 2.00 Å for Ba-Ti (△), Ba-O (○), and Ti-O (□), respectively, regarding it as a pseudocubic crystal.

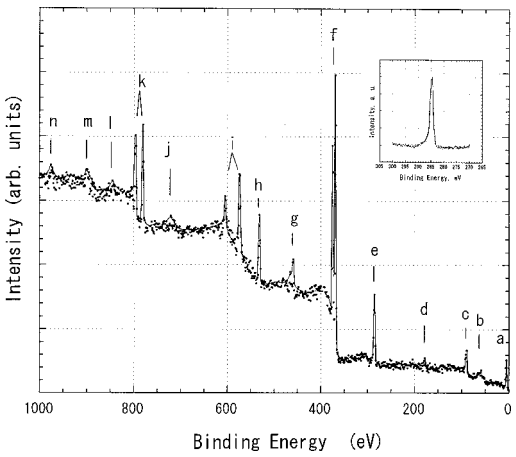

FIG. 5. Representative XPS spectrum of $BaTiO_3$ nanoparticles in the range of binding energy 0–1000 eV, where the inserted figure is a C 1s spectrum. The assignments are (a) Ag (VB), (b) Ti ($3s$,$3p$), (c) Ag ($4s$,$4p$), (d) Ba ($4p$), (e) C ($1s$), (f) Ag ($3d$), (g) Ti ($2p$), (h) O ($1s$), (i) Ag ($3p$), (j) Ag ($3s$), (k) Ba ($3d$), (l) Ti (LMM), (m) Ba (MNN), and (n) O (KLL), where VB denotes the valence band and *LMM*, *MNN*, and *KLL* represent respective Auger transitions.

relaxation for nanosize particles[13,20,21] has already occurred during the phase transition as shown in Fig. 4. Three bends exist around 1, 50, and 110 nm in the particle size. The first is related to the change from cluster calculation results to the nanoparticle experimental ones, and the second and third correspond to the beginning and end of the diffuse ferroelectric phase transition mentioned above. A dashed line indicates the expansion assuming that the nanocrystalline particle undergoes no phase transition. The graph strongly suggests that the transition suppresses the elongation of the lattice constant a with a cooperative effect in the ferroelectric phase.

B. XPS spectra and bonding character of constituent ions

Figure 5 is a XPS spectrum measured in the binding energy range from 0 to 1200 eV. This figure shows no impurities outside of carbon, as a usual contaminant, and the substrate Ag. The shift due to electrostatic charging of the sample was calibrated from the C 1s peak position to be 284.6 eV, as shown in the inseted figure. Figures 6(a), 6(b), and 6(c) illustrate XPS Ba 3d, Ti 2p, and O 1s spectra, respectively. The Ba 3d and Ti 2p spectra show very small shifts from previous data,[22] but they are considered to be genuine because of good reproducibility. The peak fitting shown in Fig. 6(c) reveals that the broad O 1s peaks consist of two components associated with hydroxide and metal oxide groups (see Table I). Peak intensity ratios of the two components, I_2/I_1, are 2.65, 1.89, 2.12, and 1.56 for the samples of the diameters $D'1$, $D'2$, $D'3$, and $D'4$, respectively, where I_1 is the integrated intensity for the metal oxide group and I_2 is that for the hydroxide group. This shows that the relative intensity for the hydroxide group tends to increase with decreasing particle size. A similar result has been very recently reported from O 1s spectra in CeO_{2-x} nanoparticles,[23] but the change of the integrated intensity ratios of 1.7 in the present case is very small in comparison

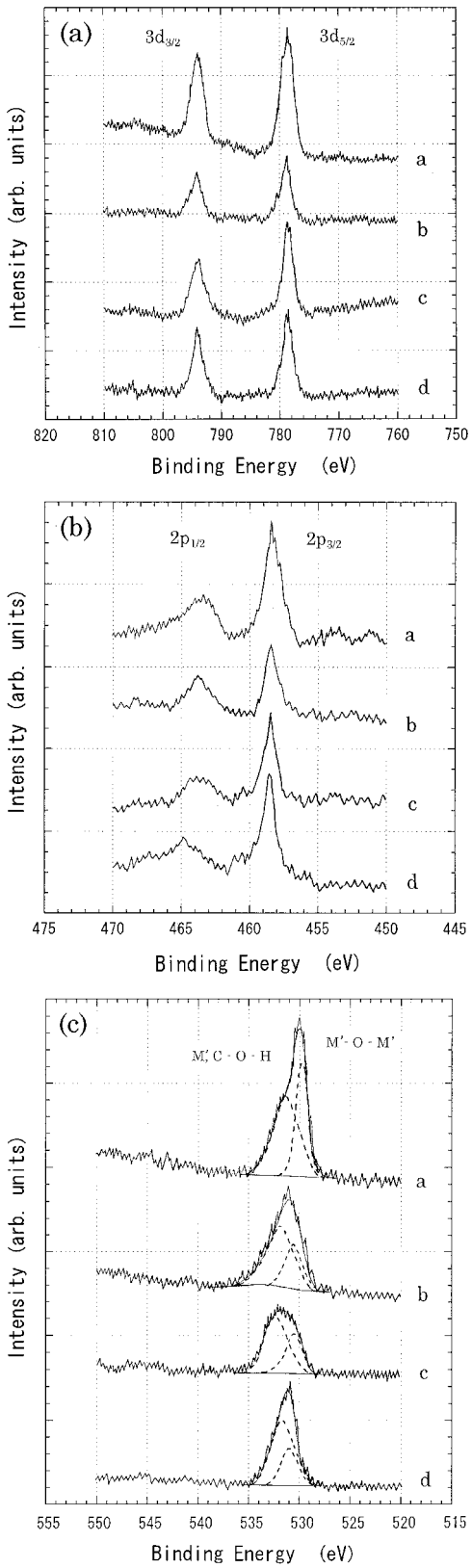

FIG. 6. (a) Ba $3d_{3/2}$ and Ba $3d_{5/2}$, (b) Ti $2p_{1/2}$ and Ti $2p_{3/2}$, and (c) O 1*s* XPS spectra, where *a*, $D'1=19\pm3$, *b*, $D'2=45\pm9$, *c*, $D'3=110\pm25$, and *d*, $D'4=350\pm80$ mm diameter particles, and $M'=$Ba or Ti.

with that for CeO_{2-x} of more than 10 times, in spite of the same lattice constant change of 1.5%. We conclude that the role of hydroxides is not important for the anomalous lattice expansion in $BaTiO_3$ nanoparticles.

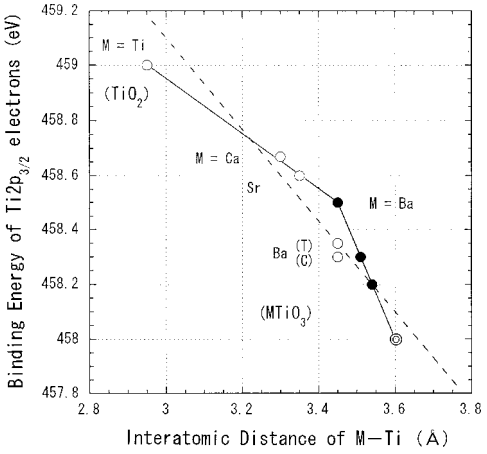

FIG. 7. Relationship between the interatomic distance (Ti-*M*) and the binding energy of T $2p_{3/2}$ electrons in TiO_2 and $MTiO_3$: the present ($M=$Ba) (●) and previous ($M=$Ti, Ca, Sr, and Ba) (○) (Ref. 27) data, and the supposed position for a cluster composed of 20 $BaTiO_3$ units (◎). The dashed line is the previous plot and the solid line is the present one. (*T*) and (*C*) following Ba denote the tetragonal and cubic phases, respectively.

Table I summarizes the position of peaks obtained from Figs. 6(a) and 6(b). Binding energies of Ba $3d_{5/2}$ electrons are constant, 779.3 eV, independent of the particle size, but the energy is different from that in BaO bulk crystals, 779.65 eV,[22] which has a sodium chloride structure and nearly ideal ionic valence of Ba +2 (the interatomic distance Ba-O is expected to be 3.00 Å from the Shannon and Prewitt ionic radii).[24] If the binding energy of Ba 3*d* electrons is affected by the polarizability of Ti as well as that of Ti 2*p* electrons by the polarizability of Ba, the energy value should increase rather than 779.65 eV. The decrease of the energy is due to the slight change from ideal ionicity in $BaTiO_3$ crystals. The binding energy of Ti $2p_{3/2}$ electrons slightly decreases with decreasing particle size below the critical size and is the same as that in bulk crystals, 458.5 eV, above the critical size, in spite of no change in the Ti-O distance (see Fig. 4). The decrease is considered to be caused by the character change of Ti-O bonds from covalent to ionic below the critical size. Such the change is consistent with previous calculations,[25,26] in which the bonding character of Ti ions is covalent in the ferroelectric phase of the bulk crystal.

Figure 7 shows a relationship between the interatomic distances *M*-Ti ($M=$Ti, Ca, Sr, and Ba) and binding energies of Ti $2p_{3/2}$ electrons in the compounds of TiO_2 and $MTiO_3$, where closed and open circles denote the present and previous results.[27] respectively. The present result suggests that the variation of the binding energy reflects the change of bonding character in Ti ions towards the cluster, while the previous paper reported that the variation is due to the change of the polarizability in cations. This figure shows also that the binding energy of 458.5 eV in the present result is better than that of 458.3 eV found in the past,[27] because the former value results in a better fitting shown by an upper solid line than the latter, which gives a least squares fitting shown by the dashed line, and a supposed position of the cluster composed of 20 $BaTiO_3$ units which gives a binding energy of 458.0 eV.

TABLE I. XPS peak positions in eV of constituent ions in $BaTiO_3$ nanoparticles obtained from ethanol suspensions, based on C $1s = 284.6$ eV.

Element \ Sample	$D'1$ (19 ± 3 nm)	$D'2$ (45 ± 9 nm)	$D'3$ (110 ± 25 nm)	$D'4$ (350 ± 80 nm)	Remark
Ba $3d_{5/2}$	779.3	779.3	779.3	779.3	779.65[a]
Ti $2p_{3/2}$	458.2	458.3	458.5	458.5	458.3[b]
O $1s$					
Ba-O-H, Ti-O-H, and C-O-H	531.7	532.0	532.3	531.7	531–533[c]
Ba-O-Ba, Ba-O-Ti, and Ti-O-Ti	529.7	530.5	530.5	530.9	529–530[c]

[a]Reference 22, p. 130.
[b]Reference 22, p. 68.
[c]Reference 22, p. 42.

C. Summary

The above results strongly suggest that the critical size corresponds to the size at which the stabilization due to ferroelectric polarization ($c > a$) is canceled and an isotropic lattice expansion begins, and the anomalous expansion is due to the change of bonding character of Ti ions, though the bond length of Ti-O is nearly constant, 2.00 Å, i.e., the distances of Ba-Ti and Ba-O extend from 3.47 to 3.60 Å and from 2.83 to 2.94 Å, respectively, with increasing electrostatic repulsion (see Fig. 4). It is noted that the interatomic distance of Ti-O is nearly constant when the bonding character changes from covalent to ionic, because the covalent radii of Ti^{4+} (VI) and O^{2-} (VI) are 1.36 and 0.66 Å, respectively,[28] whereas the ionic radii of them are 0.605 and 1.40 Å,[24] where VI denotes the six-coordination. Moreover, there exists an indirect but reasonable proof for the continuous variation of bonding character in Ti ions as shown in Fig. 7.

IV. CONCLUSION

Monodisperse $BaTiO_3$ nanoparticles were produced by hydrolyzing and heating the alkoxides. Variations of the lattice constants and core-electron states with the particle sizes were investigated by TEM and XPS, respectively. An anomalous size dependence of the lattice expansion was obtained in the wide range from bulk to cluster size. It shows two large changes corresponding to the transitions from ferroelectric to paraelectric phase and from nanoparticles to clusters. The former arises around a critical size of 80 nm, and the latter around 1 nm in diameter. It was strongly suggested by the XPS analysis that the monotonic size dependence of the anomalous expansion is due to the variation of bonding character in Ti ions from covalent to ionic. The chemical states of Ti ions in the nanoparticles will be studied by x-ray absorption near-edge structure in the near future.

ACKNOWLEDGMENTS

This work was primarily supported by a Grant-in-Aid for a seeding research from the Ministry of Education, Science, Sports, and Culture, Japan (Grant No. 10874048). The authors would like to express their thanks to Associate Professor H. Suzuki, Department of Materials Science and Technology in Shizuoka University, for his supply of the ultrafine particles. Thanks are due to professor M. Tanaka and F. Sato, Research Institute for Scientific Measurements in Tohoku University, for their support of the electron diffraction measurements. The authors are also grateful to Associate Professor K. Asami, Institute for Materials Research in Tohoku University, for his helpful discussion concerning the XPS spectra.

[1] O. Muller and R. Roy, *The Major Ternary Structural Families* (Springer-Verlag, Berlin, 1974), pp. 175–196.
[2] O. Muller and R. Roy, *The Major Ternary Structural Families* (Ref. 1), p. 221.
[3] H. D. Megaw, Nature (London) **155**, 484 (1945).
[4] H. Terauchi, Y. Yoneda, Y. Watanabe, H. Kasatani, K. Sakaue, K. Kamigaki, K. Iijima, Y. Yano, T. Terashima, and Y. Bando, Ferroelectrics **151**, 21 (1994).
[5] K. Uchino, E. Sadanaga, and T. Hirose, J. Am. Ceram. Soc. **72**, 1555 (1989).
[6] M. Alinker, H. R. Brugger, and T. Känzig, Helv. Phys. Acta **27**, 99 (1954).
[7] A. Shaikh, R. Vest, and G. Vest, IEEE Trans. Ultrason. Ferroelectr. Freq. Control **36**, 407 (1990).
[8] J. U. Muller and K. Barner, Ferroelectrics **108**, 83 (1990).
[9] T. Yamamoto, K. Urabe, and H. Banno, Jpn. J. Appl. Phys., Part 1 **32**, 4272 (1993).
[10] K. Saegusa, W. E. Rhine, and H. K. Bowen, J. Am. Ceram. Soc. **76**, 1505 (1993).
[11] S. Schlag and H.-F. Eicke, Langmuir **10**, 3357 (1994).

[12] M. Tanaka and Y. Makino, Ferroelectr. Lett. Sect. **24**, 13 (1998).
[13] K. Ishikawa and T. Uemori, Phys. Rev. B **60**, 11 841 (1999).
[14] G. Kresse and J. Furthmüller, Phys. Rev. B **54**, 11 169 (1996); Comput. Mater. Sci. **6**, 15 (1996).
[15] J. Perdew, in *Electronic Structure in Solids '91*, edited by P. Ziesche and H. Eschrig (Akademie Verlag, Berlin, 1991).
[16] R. G. Rhodes, Acta Crystallogr. **4**, 105 (1951).
[17] Y. G. Wang, W. L. Zhong, and P. L. Zhang, Solid State Commun. **90**, 329 (1994).
[18] S. Schlag and H.-F. Eicke, Solid State Commun. **91**, 883 (1994).
[19] S. Chattopadhyay, P. Ayyub, V. R. Palkar, and M. Multani, Phys. Rev. B **52**, 13 177 (1995).
[20] S. Tsunekawa, R. Sivamohan, S. Ito, A. Kasuya, and T. Fukuda, Nanostruct. Mater. **11**, 141 (1999).
[21] S. Tsunekawa, R. Sahara, Y. Kawazoe, and K. Ishikawa, Appl. Surf. Sci. **152**, 53 (1999).
[22] C. D. Wagner, W. M. Riggs, L. E. Davis, and J. F. Moulder, in *Handbook of X-ray Photoelectron Spectroscopy*, edited by G. E. Mullenberg (Perkin-Elmer Co., MN, 1979), pp. 68 and 130.
[23] S. Tsunekawa, T. Fukuda, and A. Kasuya, Surf. Sci. Lett. (to be published).
[24] R. D. Shannon and C. T. Prewitt, Acta Crystallogr., Sect. B: Struct. Crystallogr. Cryst. Chem. **25**, 925 (1969).
[25] R. E. Cohen and H. Krakauer, Phys. Rev. B **42**, 6416 (1990).
[26] R. E. Cohen, Nature (London) **358**, 136 (1992).
[27] M. Murata, K. Wakino, and S. Ikeda, J. Electron Spectrosc. Relat. Phenom. **6**, 459 (1975).
[28] L. Pauling and M. L. Huggins, Z. Kristallogr. **87**, 205 (1934).